Organization and dynamics of pyrene and pyrene lipids in intact lipid bilayers

Photo-induced charge transfer processes

Yechezkel Barenholz,* Tina Cohen,‡ Rafi Korenstein,§ and Michael Ottolenghi‡

*Department of Membrane Biochemistry and Neurochemistry, Hebrew University, Hadassah Medical School, Jerusalem; ‡Department of Physical Chemistry, Hebrew University, Jerusalem; and §Department of Physiology and Pharmacology, Tel-Aviv University, School of Medicine, Tel Aviv, Israel

ABSTRACT The dynamics of fluorescence quenching and the organization of a series of pyrene derivatives anchored in various depths in bilayers of phosphatidylcholine small unilamellar vesicles was studied and compared with their behavior in homogeneous solvent systems. The studies include characterization of the environmental polarity of the pyrene fluorophore based on its vibronic peaks, as well as the interaction with three collisional quenchers: the two membrane-soluble quenchers, diethylaniline and bromobenzene, and the water soluble quencher potassium iodide. The system of diethylaniline-pyrene derivatives in the membrane of phosphatidylcholine vesicles was characterized in detail. The diethylaniline partition coefficient between the lipid bilayers and the buffer is ~5,800. Up to a diethylaniline/phospholipid mole ratio of 1:3 the perturbation to membrane structure is minimal so that all photophysical studies were performed below this mole ratio. The quenching reaction, in all cases, was shown to take place in the lipid bilayer interior and the relative quenching efficiencies of the various probe molecules was used to provide information on the distribution of both fluorescent probes and quencher molecules in the lipid bilayer.

The quenching efficiency by diethylaniline in the lipid bilayer was found to be essentially independent on the length of the methylene chain of the pyrene moiety. These findings suggest that the quenching process, being a diffusion controlled reaction, is determined by the mobility of the diethylaniline quencher (with an effective diffusion coefficient $D \sim 10^{-7}$ cm^2 s^{-1}) which appears to be homogeneously distributed throughout the lipid bilayer. The pulsed laser photolysis products of the charge-transfer quenching reaction were examined. No exciplex (excited-complex) formation was observed and the yield of the separated radical ions was shown to be tenfold smaller than in homogenous polar solutions. The decay of the radical ions is considerably faster than the corresponding process in homogenous solutions. Relatively high intersystem crossing yields are observed. The results are explained on the basis of the intrinsic properties of a lipid bilayer, primarily, its rigid spatial organization. It is suggested that such properties favor ion-pair formation over exciplex generation. They also enhance primary geminate recombination of initially formed (solvent-shared) ion pairs. Triplet states are generated via secondary geminate recombination of ion pairs in the membrane interior. The results bear on the general mechanism of electron transfer processes in biomembranes.

INTRODUCTION

Pyrene and lipid molecules containing pyrene proved to be powerful probes for studying the molecular dynamics, the structural organization, and the polarity of assemblies which have defined hydrophobic environments. The references listed below are only representative of a very large number of publications which make use of pyrene and pyrene derivatives. These assemblies include: micelles (Waka et al., 1978; Katusim-Razem et al., 1978); lipoproteins (Massey et al., 1984); lipid vesicles (Galla and Sackman, 1974; Heresko et al., 1986, 1987); and proteoliposomes (Weiner et al., 1985).

The extensive use of pyrene and pyrene derivatives is a result of a combination between availability of various pyrene derivatives, including lipid analogues (Luisetti et al., 1979; Heresko et al., 1986, 1987; Kano et al., 1981; Massey et al., 1984; Pownall and Smith, 1989), and even more so the versatility in the properties of pyrene as a chromophore and a fluorophore. The basic processes which were extensively used are steady state fluorescence quenching (especially dynamic quenching) (Waka et al., 1980); excimer formation (Birks, 1970; Lakowicz, 1981; Galla and Sackman, 1974; Galla and Hartman, 1980; Heresko et al., 1986, 1987); exciplex and charge transfer phenomena (Mataga and Ottolenghi, 1979; Atik and Thomas, 1981; Thomas, 1980; Neumann et al., 1982; Kano et al., 1981; Waka et al., 1980).

The combination of the above properties of the pyrene moiety is very attractive for physical characterization of the various assemblies described above. Especially relevant are charge transfer processes which are markedly affected by environmental factors such as temperature, viscosity, order, external magnetic fields,

Address correspondence to Dr. Ottolenghi.

Abbreviations used in this paper: AC, Acetonitrile; DEA, Diethylaniline; ET, Ethanol; PC, Phosphatidylcholine; DPPC, Dipalmitoyl phosphatidylcholine; POPC, 1 palmitoyl 2-oleyl phosphatidylcholine; SUV, Small unilamellar vesicles; MLV, Multilamellar large vesicles; Py, Pyrene; Py-but, Pyrene butyric acid; Py-dec, Pyrene decanoic acid; Py-hexadec, Pyrene hexadecanoic acid; Py-met, Pyrene-methanol; Py-SO_3, Pyrene sulfonate; Py-val, Pyrene valeric acid.

0006-3495/91/06/110/15 $2.00

and dielectric constant. Previous work related to pyrene (acceptor)-aromatic amine (donor) systems were engaged with the kinetics of the diffusion-controlled quenching process (Waka et al., 1980; Kano et al., 1981; Neumann et al., 1982); and with the consequences of charge-transfer quenching, i.e., exciplex and ion pair formation; (Waka et al., 1980; Neumann et al., 1982). However, some basic questions remain unsolved. Especially, (*a*) the location of the quencher in the bilayer; (*b*) the quencher concentration in the bilayer; and (*c*) the degree of quencher perturbation to membrane properties.

In this paper we approach these problems by investigating photo-induced electron transfer processes involving a series of pyrene derivatives (see Scheme I) in which the length of the methylene chain determines the location of the pyrene moiety in the bilayer of small unilamellar vesicles (SUV) composed of phosphatidylcholine (PC) in its liquid crystalline state. This permits evaluation of the mechanisms associated with: (*a*) fluorescence quenching; (*b*) charge separation and recombination, as well as triplet state generation, after quenching by *N,N*-diethylaniline (DEA) as an electron donor. The results of this study bear on the structure and function of lipid bilayers in relation to: (*a*) the partition and distribution of small molecules and ions in the membrane; (*b*) the vertical and lateral membrane diffusion of the same molecules; and (*c*) the mechanism of diffusive electron-transfer processes in biomembranes.

MATERIALS AND METHODS

Pyrene (Py) was a Fluka product (99.9% purity, Prinz quality, Buchus, Switzerland). 5-(1-pyrene)valeric acid (Pry-val), 3-(1-pyrene)butyric acid (Pyr-but), pyrene-1-methanol (Py-MeOH), pyrene-1-sulphonic acid sodium salt (Py-SO_3Na) were products of Molecular Probes (Eugene, OR). All of the above were used as supplied. *N*-(1-pyrene)decanoic acid (Py-dec) and *N*-pyrene hexadecanoic acid (Py-hexdec) were a gift of Dr. A. Dagan, Department of Membrane Biochemistry and Neurochemistry, Hebrew University, Hadassah School of Medicine. KCl (Merck), KI (Baker Analar), KOH (Frutarom, Haifa, Israel), KH_2PO_4 (B & A), and Tris buffer (Sigma Chemical Co., St. Louis, MO) were all analytical grade. Solvents used were of spectroscopic grade (ethanol, dioxane and acetonitrile-Fluka, and toluene-MCB Spectroquality) and of analytical grade (chloroform; Frutarom). Bromobenzene was a Fluka product (puriss). The above solvents were used as supplied. *N,N*-diethylaniline (DEA), a BDH (Dorset, England) product, was distilled under nitrogen and later was stored in the dark under nitrogen at 4°C. Water was triply distilled through a deionizing column, over alkaline potassium permanganate, and finally over dilute phosphoric acid.

High purity soybean phosphatidylcholine (Soy PC) and egg yolk phosphatidylcholine (egg PC) were obtained from Sigma Chemical Co. High purity dipalmitoyl and 1-palmitoyl 2-oleyl phosphatidylcholine were products of Avanti Polar Lipids (Pelham, AL). All PC's were kept under nitrogen at −20°C, in the dark as chloroform solution.

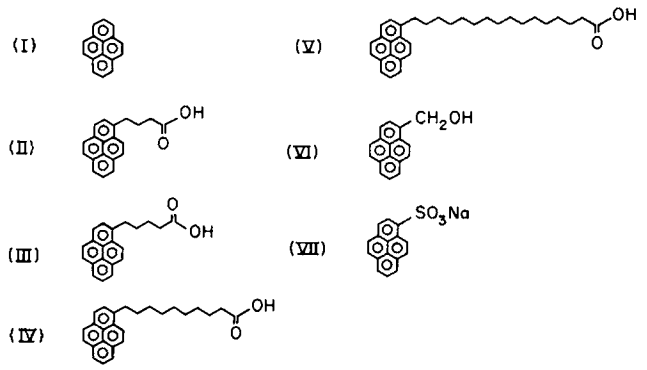

SCHEME I The molecular formulae of the pyrene derivatives used in this study: I.—Pyrene (Py); II.—Pyrene butyric acid (Py-but.); III.—Pyrene valeric acid (Py-val.); IV.—Pyrene decanoic acid (Py-dec); V.—Pyrene hexadecanoic acid (Py-hexdec); VI.—Pyrene methanol (PyMeOH); VII.—Pyrene sulfonic (Py-SO_3Na); VIII.—Pyrene tetra sulfonate [Py(SO_3Na)$_4$].

Preparation of small unilamellar vesicles

Multilamellar vesicles (MLV) were prepared in 20 mM KCl in 50 mM Tris-HCl buffer pH = 8 (buffer A) by a thin lipid hydration method as described by Bangham et al. (1967). SUV were obtained from the above MLV by ultrasonic irradiation in a bath sonicator (Laboratories Supplies Company T80801-RS, Hicksville, NY), carried out under nitrogen in the dark at 4°C till clearance of the MLV dispersion. The SUV were fractionated by differential centrifugation (Barenholz et al., 1977). For preparation of SUV containing pyrene or pyrene derivatives, the fluorophore and the phospholipid were mixed in chloroform/methanol 2:1 (by volume) at the desired mole ratio to ensure complete microscopic mixing of the components (Lichtenberg and Barenholz, 1988). The solvents were removed by flash evaporation under reduced pressure. MLV were prepared followed by ultrasonic irradiation to form SUV as described above. Aliquots of the DEA used to quench the fluorescence of pyrene or pyrene derivatives was added to the SUV as concentrated ethanolic solution at the desired concentrations. The final ethanol concentration did not exceed 0.5%. It is worth noting that DEA is volatile and therefore cannot be added during either MLV or SUV preparation.

Scanning calorimetry

Calorimetric studies were carried out on DPPC MLV dispersions using a high-sensitivity scanning calorimeter of the heat conduction type. The detailed design and operation have been described elsewhere (Barenholz et al., 1976). The lipid concentration and sample volume were 15 mM and 0.7 ml, respectively. Samples were incubated overnight in the calorimeter at the desired initial temperature to insure both thermal and system equilibrium. All experiments were in the heating mode at a scanning rate of 10° C/h. Calculations were performed on a CDC Cyber 172 computer (Control Data Corp., St. Paul, MI).

^{31}P NMR spectroscopy

Phosphorus NMR spectra of POPC MLV dispersions were obtained at 24.15 MHz using quadrature detection with a JEOL-FX60Q (Peabody, MA) Fourier-transform spectrometer operating under continu-

ous broad-band proton noise decoupling at a power of 5 W, as described before (Huang et al., 1984). A 4,000-Hz sweep width was used, and 4,000 data points were collected with 400–10,000 scans accumulated per spectrum at a delay of 1 s between pulses. A line broadening of either 10 or 5 Hz was introduced during signal enhancement for the broad asymmetrical line shapes and the narrow isotropic signals, respectively.

Spectroscopic methods

Absorption measurements were performed, at room temperature, using a spectrophotometer (Cary 219; Varian Associates, Inc., Palo Alto, CA). Fluorescence measurements were carried out on a spectrofluorimeter (MPF-44A; Perkin-Elmer Corp., Norwalk, CT). Measurements were conducted at room temperature and, as only comparative measurements were required, the spectra recorded were uncorrected. All solutions were bubbled with nitrogen for about a half hour before measurement to eliminate free oxygen. The excitation wavelength was adjusted for each fluorescence probe examined so as to keep the absorption of the solution low (0.1–0.16 O.D.) and thus ensure homogeneous absorption of the excitation light.

Time-dependent fluorescence decay curves, for the calculation of fluorescence lifetimes and transient absorption measurements, were carried out using an Avco-Everett N_2 laser (337.1 nm, 8ns, 0.5 mJ) in a previously described setup (Goldschmidt et al., 1970; Neumann et al., 1982). Kinetic traces of phototransients were digitized and averaged using a combined Biomation 8100 (digitizer)-Nicolet 1170 (signal averager) system and displayed on an XY recorder. Acceptable signal-to-noise ratios were usually obtained by averaging at least 32 pulses. All systems investigated in the present work were highly reversible. Even after 10^3 laser pulses no changes could be detected either in the absorption spectra of the solutions or in the magnitude or kinetics of the absorbance changes in the photolysis experiments. In some cases, especially for comparing the life time in the absence (τ_0) and presence (τ) of DEA, the emission life time was measured as described by Barenholz et al. (1978) using an excitation band of 3–10 nm. Monomer emission was determined in the range of 370–390 nm using a combination of KV 370 + 3986 filters. The agreement between the two methods was very good (compare τ_0 of 135 ns obtained by the first method; Table 1) with 140 ns obtained by the second method, for pyrene in egg PC SUV.

RESULTS

I. Effect of DEA on lipid bilayers

Most of the work described in this paper is based on the interaction of DEA with pyrene and pyrene labeled lipids in lipid bilayers. Therefore, special efforts were devoted to studying the DEA bilayer/medium partition coefficient (K_p) as well as the mode and extent of bilayer perturbation caused by DEA.

(i) Partition of DEA between lipid bilayers and medium (K_p)

The overall partition coefficient of DEA between egg PC, SUV, and the aqueous phase (K_p) was determined by equilibrium dialysis (Sikaris et al., 1981). For this 1 ml of egg PC SUV dispersion buffer pH 8.0 containing 20 mM KCl (buffer A) was placed in 1 cm diam visking dialysis tubing bags. The bags were introduced into 4 ml buffer A in glass test tubes. Either 1 or 3 mM egg PC was used. DEA (0.1–0.25 μmol) was added to the external buffer solution. In a parallel set of experiments the DEA was added inside the dialysis bags containing the SUV. The dialysis was performed at 20°C. The external buffer was stirred continuously using magnetic stirrers. The incubation was terminated when the DEA concentration in the external buffer reached a plateau. This was determined from its absorption at 244 nm (Sikaris et al., 1981). In all cases, 2 h were sufficient to reach equilibrium. It was found that the permeability through the membrane of the dialysis bag was the rate limiting factor in the equilibration process. Aliquots of the SUV dispersion and of the external buffer were removed and were diluted with ethanol and buffer to give a final solution of

TABLE 1 Kinetic parameters for the quenching of pyrene and pyrene derivatives by iodide and bromobenzene in homogeneous acetonitrile (AC) or ethanol (ET) solution and in PC vesicles

	Iodide ion					Bromobenzene				
Fluorophore	System	τ_0, *ns*	$k_q \times 10^{-7}$ $M^{-1}s^{-1}$	$\frac{k_q}{k_q(AC)}$	$\frac{k_q}{k_q(AC)_{norm}}$	System	τ_0, *ns*	$k_q \times 10^{-7}$ $M^{-1}s^{-1}$	$\frac{k_q}{k_q(ET)}$	$\frac{k_q}{k_q(ET)_{norm}}$
Pyrene	AC	295	751	0.0066	1.0	ET	162	1.5	74	1.0
(I)	PC	135	5			PC	135	112.0		
Py-val.	AC	258	261	0.0150	2.5	ET	184	1.6	40	0.5
(III)	PC	140	4			PC	140	64.0		
Py-dec.	AC	165	308	0.0065	1.0	ET	220	1.2	66	0.9
(IV)	PC	134	2			PC	134	80.0		
Py-hexadec.	AC	131	472	0.0065	1.0	ET	223	0.9	160	2.1
(V)	PC	133	3			PC	133	148.0		
Py-SO_3Na	—	—	—			ET	212	1.5	78	1.0
(VII)	PC	60	110	—	—	PC	57	117.0		

The parameter ratios $[k_q/k_q\,(AC)]_{norm}$, or $[k_q/k_q(ET)]_{norm}$, are normalized with respect to Py which is taken as a unity reference.

ethanol/buffer of 9:1 (vol/vol). This procedure ensured identical molar extinction for all samples. The ethanol is required to solubilize the SUV to eliminate the disturbance by SUV turbidity. The absorbance of DEA in the range of 240–280 nm was monitored. The integrated spectra were used to determine DEA concentrations. The values obtained for the external buffer solution and SUV dispersion were corrected using systems without DEA.

The partition coefficient was calculated using the equation described by Sikaris et al. (1981):

$$\frac{M_L}{M_A} = \frac{[Q]_L \times V_L}{[Q]_A \times V_A} = K_P \frac{V_L}{V_A} \quad (1)$$

$$K_P = \frac{M_L \times V_A}{M_A \times V_L}, \quad (2)$$

where K_P is the partition coefficient of DEA between egg PC, SUV, and buffer A; $[Q]_L$ is the concentration of DEA in the lipid phase (SUV); $[Q]_A$ is the concentration of DEA in the aqueous phase; V_L is the volume of the lipid phase; V_A is the volume of the aqueous phase, in good approximation it is identical to the total volume of the system (V_T); M_L is the amount of DEA in the lipid phase, which was obtained by subtracting the content of DEA present in 1 ml external buffer from the total amount of DEA inside the dialysis bag (1 ml); M_A is the amount of DEA in the total aqueous phase (4 ml external buffer plus 1 ml buffer inside the dialysis bag). V_L was calculated from the following equation:

$$V_L(\mu l) = P(\mu mol) \times MW(mg) \times V(ml/g). \quad (3)$$

$P(\mu mol)$ is the PC content expressed in μmoles. $MW(mg)$ is the molecular weight of egg PC expressed in milligrams (0.75 mg). $V(ml/gr)$ is the partial specific volume of egg PC SUV. This was determined to be 0.984 ml/gr at 20°C (Barenholz et al., 1977). For 1 μmol egg PC V_L is equal to 0.738. A K_P value of $5.8 \pm 1.6 \times 10^3$ for the partition of DEA between egg PC SUV and buffer A was determined from the equilibrium dialysis experiments. Identical values were obtained for DEA present inside and outside the dialysis, indicating that the systems are indeed in equilibrium. Based on the above K_P value, in a system containing 1 mM PC (a concentration which was used for most of the experiments described in this study), 81% of the DEA is located in SUV whereas 19% is in the aqueous phase.

(II) Perturbation of lipid bilayers by DEA

The relatively high K_P value found for DEA implies a high concentration in the lipid bilayer, which may cause major dose-dependent bilayer perturbations. Our goal was to investigate such perturbations and their dependency on the DEA/lipid ratio, to perform photophysical studies under minimal perturbations. The latter were characterized by four independent methods: (*a*) turbidity; (*b*) electron microscopy (EM); (*c*) differential scanning calorimetry (DSC); and (*d*) ^{31}P-nuclear magnetic resonance (P-NMR). Soy PC and egg PC SUV were used for turbidity studies; soy PC was used for the electron microscopy studies. In both systems above a DEA/lipid ratio of 1.0 (for 1 mM PC) a major increase in turbidity appeared. Electron micrographs of soy PC SUV revealed formation of large aggregates and possibly fusion. It is possible that under such high DEA/lipid ratio and due to the high K_P value the lipid becomes saturated with DEA, its low water solubility causes macroscopic phase separation from the aqueous phase leading to increase in turbidity (DEA droplets). Also working at DEA/lipid ratio higher than 1.0 causes sharp appearance of exciplex emission (as described below in section II, Fluorescence quenching). The DEA saturation level promotes vesicle aggregation and possibly fusion. Therefore, all other experiments were done at [DEA]/[lipid] ratio < 1.0.

^{31}P-NMR. Chemical shift anisotropy of P-NMR is one of the major analytical methods to determine transformation from lamellar to nonlamellar type of organization of phospholipid aggregates (Sackman, 1983; Cullis et al., 1985; Tilcock, 1986). Therefore, as a representative of a system in liquid crystalline state, we compare MLV of 1-palmitoyl-2-oleyl PC (POPC) with and without DEA using DEA/POPC ratio of 1:3 and 1:1. All three samples gave identical spectra characteristic to lamellar structure, suggesting that DEA does not induce lipid phase transformation.

Differential scanning calorimetry. For this we used MLV of dipalmitoylphosphatidylcholine (DPPC) which have a defined thermotropic behavior with respect to the Tm of their main and pretransitions, as well as a high cooperativity of the main transition (Suurkuusk et al., 1976). Minor perturbations to the above characteristics are easily determined from the thermograms characterizing MLV containing the perturbant (Ben Yashar et al., 1987). The DSC was performed under two DEA/lipid mole ratio (1:3 and 1:1) using a DPPC concentration of 15 mM. From such thermograms it is evident that DEA affects the thermotropic behavior of DPPC and that the effect is strongly dependent on the DEA/lipid mole ratio. At a 1:3 mole ratio DEA causes disappearance of the pretransition, broadening of the main gel to liquid-crystalline phase transition and therefore decreases in its cooperativity (compare Fig. 1 *A* with Fig. 1 *B*). This broadening is asymmetric and is larger at the low temperature side of the endotherm, suggesting that DEA preferentially concentrates in the more fluid

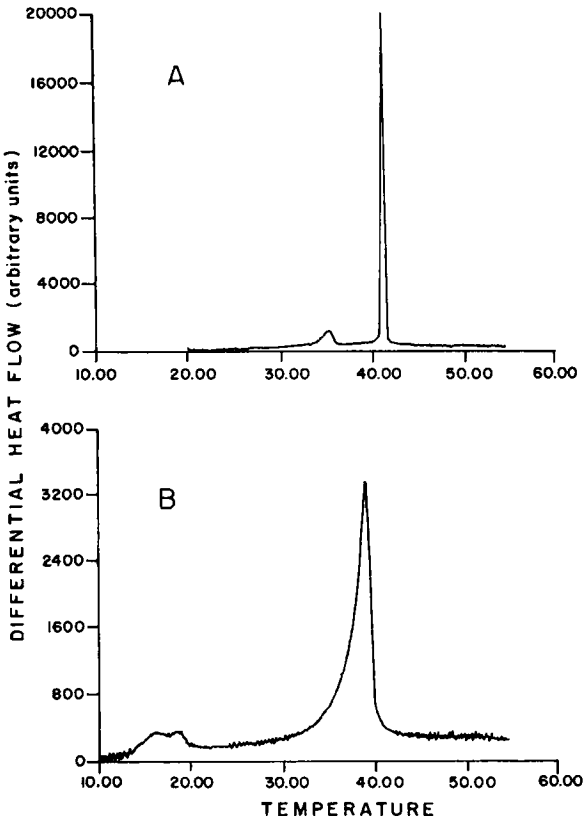

FIGURE 1 Thermograms obtained by high sensitivity differential scanning calorimetry of multilamellar large vesicles of dipalmitoyl phosphatidylcholine (DPPC) (*A*) and DPPC/DEA 3:1 (mol/mol). (*B*) The DPPC concentration was 15 mM, in 10 mM potassium phosphate buffer (pH 8.1), containing 50 mM KCl and 0.1 mM K-EDTA. For more details see text.

liquid-crystalline phase, opposite to what was found for trans parinaric acid (Ben Yashar et al., 1987). This assumption is also supported by the decrease of Tm from 41.4°C, for plain DPPC MLV, to 39.0 DPPC MLV containing 25 mol % DEA. However, there is no change in number of DPPC molecules undergoing phase transition because ΔH calculated from the area under the endotherm of the main transition remain unchanged (8.5 ± 0.2 Kcal mol^{-1}). At equimolar DEA/DPPC ratio the perturbation is much larger (data not shown). The phase transition becomes much broader (25–37°C) and a new narrow component appears with Tm of 26°C. The structural significance of these drastic changes in the thermogram is not yet clear. Similar studies cannot be carried out with either egg PC or POPC vesicles due to their low Tm. However, the fact that DEA prefer the liquid-crystalline phase suggests that the data obtained for the DPPC system are applicable to other systems when present in liquid-crystalline phase.

In conclusion it is clear that although DEA is a perturbant of lipid bilayers, at least up to equimolar concentration with the phospholipid, it does not cause any major transformation to nonlamellar types of organization. It affects the thermotropic behavior of lipids. However, when its concentration in the lipid bilayer is ≤ 25 mol %, this effect is rather small.

II. Fluorescence quenching of pyrene and pyrene derivatives in bilayers of lipid vesicles

Quenching of the fluorescence of 5×10^{-5} M of pyrene derivatives (molecules I–VII, Scheme I) by DEA was investigated both in egg phosphatidylcholine and soybean phosphatidylcholine vesicles at 25°C. As shown in Fig. 2 *a* quenching by DEA was found to fairly obey the Stern-Volmer relationship (Stern and Volmer, 1919), $(I_0/I) - 1 = K_{sv}[\text{DEA}]$, up to almost 70% quenching which was obtained at [DEA] = 4×10^{-4} M and [PC] = 1×10^{-3} M. I_0 and I are the relative fluorescence intensities in the absence and in the presence of DEA, respectively, and K_{sv} is the Stern-Volmer constant related to the quenching rate constant, k_q, and to the fluorescence lifetime, τ_0, via $K_{sv} = k_q\tau_0$. To show that the observed quenching process is dynamic in nature, we performed representative experiments in which the life time ratio τ_0/τ (τ_0, in the absence, and τ in the presence of DEA) was compared with the intensity ratio I_0/I. For example, in the case of [DEA] = 2.5×10^{-4} M and 1×10^{-3} M egg PC. We found $\tau_0 = 140$ ns and $\tau = 34.1$ ns, yielding a τ_0/τ value of 4.1 which is almost identical to the value of 4.2 ± 0.2 that was measured for I_0/I. The latter value is in a good agreement with the data described in Fig. 2 *a*. The observation is in keeping with a diffusion-limited quenching mechanism. In such relatively dilute fluorophore systems the emission spectrum is almost exclusively due to the monomer bands in the 365–425 nm range. (A very weak excimer fluorescence peaking around 480 nm is observed only in the case of Py-hexdec). No changes in the emission spectra of the pyrene moiety due to quenching were observed within the above DEA concentration range. One should especially note that in this range the quenching process is not associated with the appearance of the characteristic 460 nm fluorescence of the pyrene-DEA exciplex which accompanies the reaction in nonpolar homogeneous solutions (For a review see Mataga and Ottolenghi, 1979). Analogous exciplex bands were observed by us for molecules II–V in toluene (see Fig. 3). We note, however, that upon increasing the DEA concentration in vesicle systems to above 10^{-3} M, (a [DEA]/[lipid] > 1.0), an emission around 460 nm, attributable to the exciplex appeared as was demonstrated for pyrene (see Fig. 3 *d*).

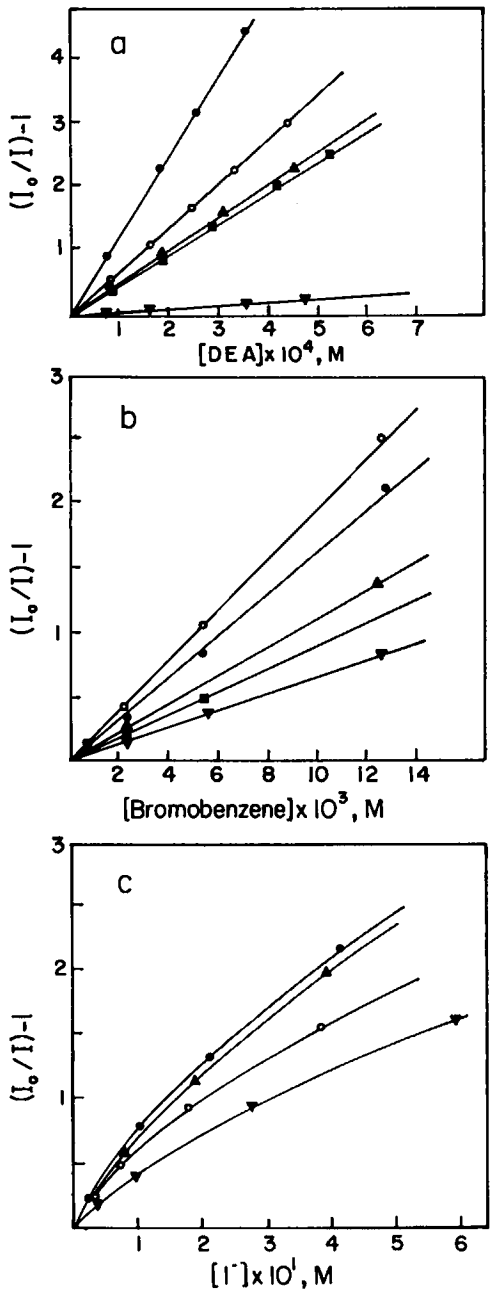

FIGURE 2 Stern-Volmer plots of pyrene and pyrene derivatives quenched by DEA, bromobenzene and iodide in small unilamellar vesicles (I_0 and I represent the relative fluorescence intensity in the absence and in the presence of the quencher, respectively): (*a*) soybean phosphatidylcholine vesicles; quencher DEA ●—I (pyrene); ▲—II (Py-but); ■—III (Py-val); ○—VI (Py-met); ▽—VII (Py-SO_3). Lipid concentration: 1 × 10^{-3} M, pH 7 (phosphate buffer) 100 mM KCl. Probe concentration 1.2 × 10^{-5} M. (*b*) Egg phosphatidylcholine vesicles; quencher Bromobenzene ●—I (pyrene); ■—III (Py-val); ▲—IV (Py-Dec); ○—V (Py-hexdec); ▼—VII (Py-SO_3). Conditions as in *a*. Ethanolic solution (0.95 M) of bromobenzene was used; highest ethanol concentration per sample was 1%. (*c*) Egg PC vesicles, quencher potassium iodide ●—I (Py); ▲—III (Py-val); ▼—IV (Py-Dec); ○—V (Py-hexadec). Lipid concentration: 1 × 10^{-3}; Tris buffer (50 mM), pH 8; 20 mM KCl, probe concentration 5 × 10^{-6} M.

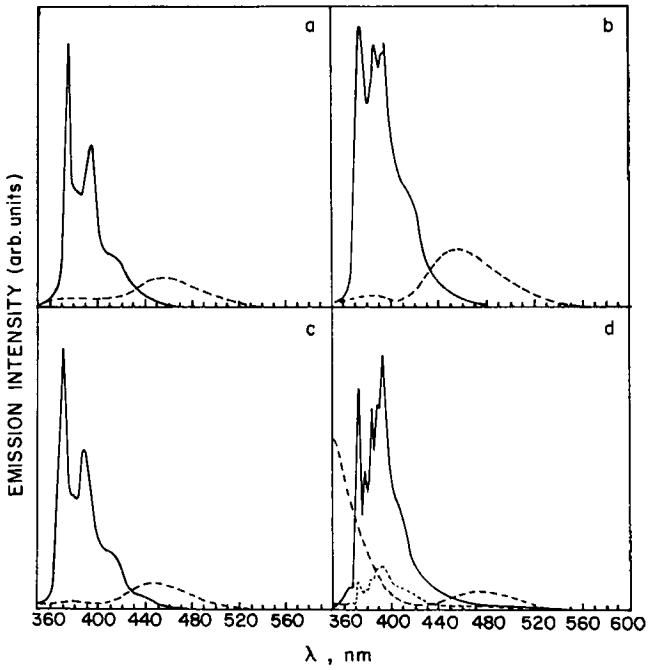

FIGURE 3 Fluorescence spectra of pyrene and pyrene derivatives in toluene (*a–c*) and PC (*d*) quenched by DEA: in all cases the solid lines represent the fluorescence spectrum in the absence of DEA. (*a*) Py-Val (III) in toluene: broken line, in presence of 5.2 × 10^{-2} M DEA. (*b*) Py-dec (IV) in toluene: broken line, in presence of 5.2 × 10^{-2} M DEA. (*c*) Py (I) in toluene: broken line, in presence of 1.25 × 10^{-2} M DEA. (*d*) Py (I) in PC: dotted line (. . .), in presence of 4.2 × 10^{-4} M DEA. Broken line (---), in presence of 2.1 × 10^{-2} M DEA.

The phenomenon was accompanied by an increase in the scattering of the SUV suspensions, reflecting major structural changes in the SUV as confirmed by negative staining electron microscopy and DSC data (see above). This was also followed by negative deviations (leveling-off) in the Stern-Volmer relationship. We therefore conclude that the conditions in which exciplex are formed in the vesicles are irrelevant to intact bilayers and cannot be used for membrane studies.

For comparative purposes, fluorescence quenching of the above molecules by DEA was also investigated in homogeneous acetonitrile solutions. Table 2 gives the main quenching parameters for both PC SUV and acetonitrile systems. The measured emission lifetime in the absence of the quencher is presented along with the bimolecular quenching rate constants, k_q. In the vesicles the latter parameter was evaluated using the overall DEA concentration in the membranes, calculated on the basis of the measured values of K_p. The data are summarized in the form of the parameter ratio $k_q/k_q(AC)$ which reflects the quenching efficiency in the lipid bilayer (k_q) relatively to the same process in

TABLE 2 **Kinetic parameters for the quenching of pyrene and pyrene derivatives by DEA in deaerated acetonitrile (AC) in soybean PC (SB) and egg PC vesicles (PC)**

Fluorophore	System	τ, ns*	$k_q \times 10^{-10}$, $M^{-1} s^{-1}$	$k_q/k_q(AC)$‡	$[k_q/k_q(AC)]_{norm}$§
Py (I)	AC	295	1.8	1.0	1.0
	PC	135	9.1	5.1	1.0
	SB	125	10.8	6.0	1.2
Py-but. (II)	AC	153	1.8	1.0	1.0
	SB	88	6.1	3.4	0.6
Py-Val. (III)	AC	258	1.7	1.0	1.0
	PC	140	5.9	3.5	0.7
	SB	124	4.0	2.4	0.4
Py-dec. (IV)	AC	165	1.5	1.0	1.0
	PC	134	10.5	7.0	1.4
Py-hexadec. (V)	AC	131	2.1	1.0	1.0
	PC	133	10.3	4.9	1.0
Py-MeOH (VI)	AC	217	1.7	1.0	1.0
	SB	139	4.9	2.9	0.5
Py-SO_3NA (VII)	AC	192	1.3	1.0	1.0
	SB	55	0.8	0.6	0.1

*Fluorescence lifetime in the absence of DEA.
‡k_q(AC) is the value of k_q in acetonitrile.
§The parameter ratio $[k_q/k_q(AC)]_{norm}$ is normalized to its value for Py in PC which is taken as unit.
For the Roman numbers refer to Scheme I. System: AC, acetonitrile; PC, egg PC; SB, soybean PC.

homogeneous acetonitrile solutions k_q(AC). We note that in the vesicle systems k_q is an apparent rate constant related to the analytical concentration of the membrane-bound quencher in the total system and not to its actual concentration within the lipid bilayer. It is evident that the apparent k_q in the vesicle is of the same order of magnitude as in the acetonitrile homogeneous solutions. However, correction for the actual membrane volume (see Discussion and Table 3) demonstrate that the effective k_q in the membrane is two orders of magnitude lower than k_q in acetonitrile. It is also worth noting that the lowest k_q/k_q(AC) ratio was obtained for the probe Py-SO_3Na (compound VII, Scheme I), which should be located near the lipid water interface and therefore may be the least available for quenching by DEA.

Fluorescence quenching experiments were also carried out using two heavy atom quenchers. The iodide ion, characterized by a high affinity to the aqueous phase, and bromobenzene, whose solubility in the membrane phase is expected to resemble that of DEA. Quenching of pyrene, pyrene valerate, pyrene decanoate, pyrene hexadecanoate, or pyrene sulfonate in egg PC SUV by bromobenzene, added to suspensions of PC vesicles yielded linear Stern-Volmer plots (Fig. 2 *b*). In the case of the iodide ion the Stern-Volmer plots show deviations from linearity (Fig. 2 *c*). The quenching rate constants obtained from the initial slopes of both sets of plots are given in Table 1, in comparison to those measured in homogeneous acetonitrile or ethanol solutions.

TABLE 3 **Diffusion coefficients obtained using Vanderkooi and co-workers' model for two-dimensional diffusion**

Fluorophore*	k_q(eff)‡	D‡
	$M s^{-1}$	$cm^2 s^{-1}$
Py	2.7×10^8	7.0×10^{-7}
Py-val.	1.7×10^8	4.4×10^{-7}
Py-dec	3.1×10^8	8.0×10^{-7}
Py-hexdec	3.35×10^8	8.6×10^{-7}

*For the exact structure see Scheme I.
‡For the method of calculation see Discussion.

III. Vertical localization of the pyrene fluorophore in lipid bilayers

It is well established that in homogeneous solutions the fine structure of the pyrene monomer fluorescence is markedly affected by the polarity of the solvent (Nakajima, 1971; Dong and Winnik, 1982). Polar solvents enhance the intensity of the 0-0 band (I_I), whereas there is a smaller but opposite effect on band III (see Fig. 4 *a*). Thus, the I_I/I_{III} intensity ratio constitutes an effective indicator of the environmental polarity, which has been applied for probing various (nonhomogeneous) microen-

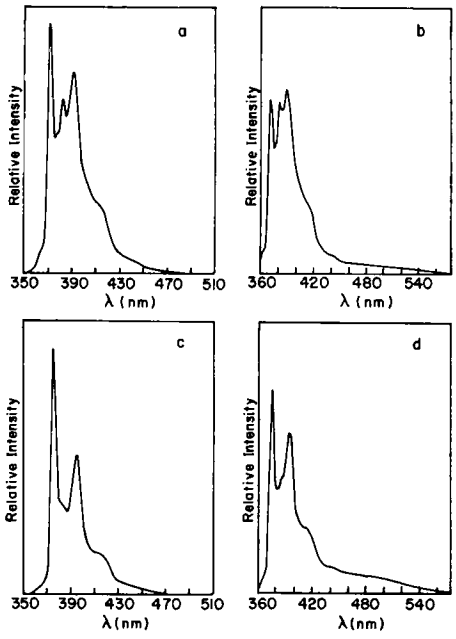

FIGURE 4 Steady-state fluorescence spectrum of 5×10^{-6} M pyrene in dioxane (*a*) and egg PC SUV (1×10^{-3} M PC) (*b*); *c* and *d* are the same as *a* and *b* but for the pyrene decanoic acid derivative.

vironments (e.g., see Kalyanasundaram and Thomas, 1977; Winnik et al., 1987 and references therein).

Fig. 4 compares the fluorescence vibronic structure of pyrene in egg PC SUV with that observed in homogeneous dioxane solution. The value of 1.06 observed for the I_I/I_{III} intensity ratio in the bilayer should be considered on the basis of a calibration curve, plotting I_I/I_{III} vs. Dimroth's E_T polarity parameter for a series of 25 aprotic solvents (Dong and Winnik, 1982). The value in the bilayer is indicative of a relatively low polarity environment, similar to that characteristic of low dielectric constant solvents, such as bromobenzene or chlorobenzene (E_T = 34–38). Unfortunately, a similar analysis could not be carried out with all other pyrene derivatives employed in the present work. As shown in the case of Py-dec (Fig. 4, *c* and *d*), the presence of the alkyl chain results in a relatively simple vibronic structure, with only two major peaks (374 and 394 nm), characterized by a solvent-independent intensity ratio.

IV. Pulsed laser photolysis

Pulsed laser photolysis of pyrene (I), pyrene valerate (III), pyrene decanoate (IV), and pyrene hexadecanoate (V) were carried out in egg PC SUV dispersions using a probe to lipid molar ratio of 1:25. The experiment was carried out in the absence and in the presence of DEA. Control experiments were also performed with vesicles containing only the quencher DEA. Transient spectra observed after exposing DEA-free suspensions of the fluorophores in PC to the laser pulse are shown in Fig. 5. The general patterns are essentially the same for all four molecules, reflecting the characteristic bands of the corresponding triplet states (^{3}Py) around 420 nm, as well as a secondary maximum around 455 nm. The latter band is left as a residual absorption (~1 ms) after the faster triplet decay (~1 μs). Identification of the 455 nm band as due to the corresponding radical cations of the pyrene moiety is supported by their absorption maxima (455 nm in the case of Py^+ [Grellmann et al., 1970]) and by the presence of a broad band around 680 nm (measured after more than 50 ns) attributable to the solvated electron, e_{aq}^- (Anbar and Hart, 1968; Birks, 1970). On the basis of the values of the extinction coefficients of Py^+ ($\in[Py^+]$ [455 nm] = 4×10^4 M^{-1} cm^{-1} [Grellman et al., 1970]) and of e_{aq}^- ($\in[e_{aq}^-]$ [680 nm]) = 1.7×10^4 M^{-1} cm^{-1} the data of Fig. 5 indicate that Py^+ and e_{aq}^- are formed stoichiometrically in keeping with the photoionization process

$$Py \xrightarrow{h\nu} Py^+ + e_{aq}^-$$

in which Py represents pyrene or its derivatives.

The yield of ^{3}Py* in the vesicles (ϕ_f^v) is lower than that observed in a dilute (excimer free) ethanol solution (ϕ_f^s) by approximately a factor of 7. The effect is qualitatively accounted for by the reduced intrinsic monomer fluorescence lifetime of Py in the vesicle (τ_f^v = 120 ns as compared with τ_f^s = 320 ns in a dilute ethanol solution) and by the fact that intersystem crossing (ISC) in the

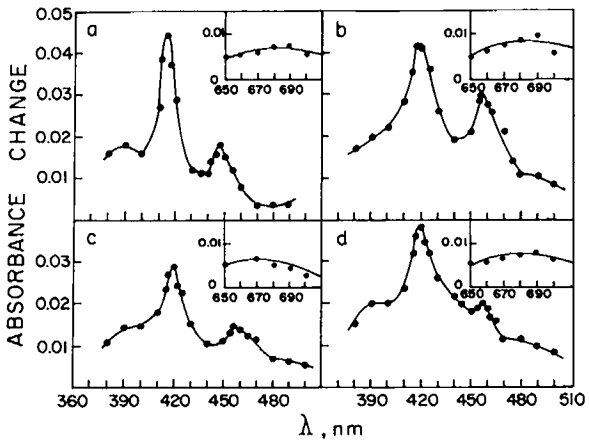

FIGURE 5 Transient spectra observed in the pulsed laser photolysis of (*a*) pyrene (I); (*b*) Py-hexadecanoic acid (V); (*c*) Py-valeric acid (III); (*d*) Py-decanoic acid (IV) in the absence of DEA as quencher. Lipid concentration: 10^{-3} M, 50 mM Tris buffer pH 8, 20 mM KCl. Probe concentration: 4×10^{-5} M DEA 1.7×10^{-3} M.

exciplex is only 20% of that characterizing $^1Py^*$ (Birks, 1970), i.e.: $\phi_i^v/\phi_i^s = \tau_f^v/\tau_f^s \simeq \phi_f^m + 0.2\,\phi_f^{ex}$, where $\phi_f^m \simeq 0.7$ and $\phi_f^{ex} = 1 - \phi_f^m \approx 0.3$ are, respectively, the relative yields of monomer and excimer fluorescence in the vesicle system. (It is assumed that the ISC rates are independent of the environment.)

Control experiments carried out with DEA in fluorophore-free liposomes show the formation of a broad absorption around 470 nm (Neumann et al., 1982). The spectrum is characteristic of the DEA^+ radical ion (Aalbersberg et al., 1959), and is thus attributed to the photoionization process:

$$DEA \xrightarrow{h\nu} DEA^+ + e_{aq}^-.$$

Taking into account the relative initial absorbance at 337.1 nm and the extinction coefficients of the respective radical cations, the yield of the DEA photoionization process is found to be higher by a factor of ~100 relative to those of pyrene and its derivatives.

The results of laser photolysis experiments carried out in mixed DEA pyrene or pyrene derivatives in liposome systems are shown in Fig. 6. The presence of 7.5×10^{-4} M DEA quenches 95% of the pyrene (4×10^{-5} M) fluorescence in the above liposomes. The "initial" spectrum in Fig. 6 (recorded after 50 ns) is composed of the characteristic bands of $^3Py^*$ (−420 nm), Py^- (500 nm),

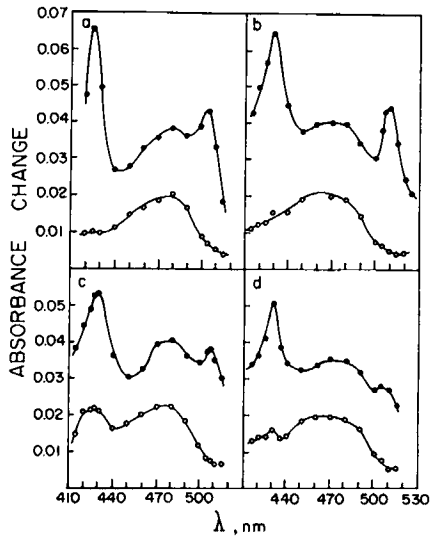

FIGURE 6 Transient spectra observed in pulsed laser photolysis of Py (*a*), pyrene valeric acid (*b*), pyrene decanoic acid (*c*), pyrene hexadecanoic acid (*d*), in the presence of DEA: (*full circles*) 50 ns after the laser pulse. (*Open circles*) 10 μs after the laser pulse. Conditions as in Fig. 3.

DEA^+ (~465 nm), and e_{aq}^- (in the range 650–750 nm, not shown). The relative amplitudes and the decay patterns of the various species are given in Table 4. The 500 and 470 nm bands of Py^- and DEA^+, respectively, decay simultaneously with an initial half-life of $\tau_{1/2} = 0.5$ μs. The relative amplitudes of the absorbance fractions decaying at 500 and 465 nm are 4:1, in keeping with the ratio between the respective extinction coefficients (Grellmann et al., 1970) $\in(Py^-)$ (500 nm) $\approx 5 \times 10^4\ M^{-1}\ cm^{-1}$ and $\in(DEA^+)$ (465 nm) $\approx 1 \times 10^4\ M^{-1}\ cm^{-1}$. It is thus evident that we are observing the recombination of Py^- and DEA^+. Following the decays of the triplet and of the radical ions, a residual band characteristic of DEA^+ (Fig. 6) is observed, very slowly decaying with a half-life of ~80 ms. Because the process is not accompanied by a matching absorbance decay at 500 nm it is suggested that the residual amount of DEA^+ is due to the photoionization of DEA, yielding DEA^+ and e_{aq}^-. This is in keeping with the matching absorption of e_{aq}^-. However, as in the case of the

$$Py \xrightarrow{h\nu} Py^+ + e_{aq}^-$$

process reported above, the solvated electron decay ($\tau_{1/2} = 0.6$ μs) is much faster than that of the residual DEA^+ cation. The latter process is thus attributed to the reaction between DEA^+ and an unidentified reduction product of the solvated electron. It is worthwhile noting that the residual DEA^+ transient absorption in the mixed Py-DEA liposome system (Fig. 6) is considerably higher than that recorded in the corresponding pyrene-free system. In view of the pronounced inner filter effect due to the high pyrene absorbance (≈ 1.2 in 1 cm at 337 nm) in the mixed system, it is evident that in this case the direct photoionization of DEA cannot account for more than a few percent of the (residual) DEA^+ and of e_{aq}^-. A

TABLE 4 Changes in adsorption (*A*) and initial half-lifetimes ($\tau_{1/2}$) of the transient species formed from pyrene (and its derivatives) + DEA in PC vesicles

Probe molecules	Triplet, $^3Py^*$		Py^- radical anion		Residual radical cation, DEA^+	Ratio of yields
	A	$\tau_{1/2}$	*A*	$\tau_{1/2}$	*A*	$^3Py^*:Py^-$
		μs		s		
Py	0.065	1.1	0.043	0.5	0.020	1:0.7
Py-val	0.053	6.0	0.038	0.7	0.023	1:0.7
Py-dec	0.051	3.8	0.028	0.9	0.020	1:0.6
Py-hexdec	0.065	2.3	0.044	0.5	0.021	1:0.7

plausible explanation involves the following sequence of events:

$$Py \xrightarrow{h\nu} Py^+ + e_{aq}^-$$

$$Py^+ + DEA \longrightarrow DEA^+ + Py.$$

Figs. 5 and 6 show that except for small differences in the location and relative amplitudes the absorption maxima of $^3Py^*$ and Py^-, the main photochemical patterns reported for pyrene are also observed in the case of the three carboxylic acid derivatives Py-val, Py-dec, and Py-hexdec as well as for Py-SO_3Na. The relative yields of the various photointermediates are summarized in Table 4.

DISCUSSION

Quenching process

We studied the fluorescence and photochemistry of pyrene and various pyrene containing lipids in bilayers of egg or soybean phosphatidylcholine small unilamellar vesicles. Quenching and recombination processes were the main tools in this study. Among the various quenchers used, the quenching by DEA was characterized in most details. Firstly, the DEA actual concentration in the lipid bilayers was determined, then its effect on the bilayer integrity was characterized and the concentration in which bilayer perturbation is minimal was determined. No previous attempts to define such systems were reported. Comparison between the liposomal systems and homogeneous solutions were used throughout this study.

Information on the exact location of fluorophores and quenchers in the SUV bilayer is a fundamental prerequisite for understanding the quenching mechanism. On the basis of proton NMR data, Gratzel et al. (1974) have shown that the location of the aromatic moiety of pyrene butyrate and pyrene sulfonate (Scheme I) in micellar systems is qualitatively determined by the chain length which is related to the distance from the polar acid residue located at the lipid-water interface. Similar experiments were performed by Vanderkooi et al. (1975) in phospholipid vesicles. Direct evidence showing that the carboxylic acid group in the series of w-pyrene carboxylic acids (II–V, Scheme I) is anchored at the lipid bilayer-water interface, with the pyrene chromophore extending into the membrane interior to an extent determined by the length of the methylene chain, has been obtained by Luisetti et al. (1979). Their conclusion is based on the observation that quenching of pyrene, pyrene butyrate, and pyrene hexadecanoate by *X*-nitroxide stearates (X = 5, 12, 16) is optimal when the spin label quencher is situated at the same chain length distance from the polar head group as is the pyrene moiety in the probe. These conclusions will serve as the basis of our analysis of the quenching reactions by DEA, bromobenzene, and iodide. Regarding DEA, its membrane/aqueous medium partition coefficient ($K_p = 5.8 \times 10^3$) is higher by a factor of ~44 relative to that of homologous dimethylaniline (DMA) in similar systems (Sikaris et al., 1981) which have been employed for photophysical investigations (Waka et al., 1980). The difference between the two is explained by the longer alkyl chains of the DEA which increase its hydrophobicity. This suggests that DEA is superior over DMA for membrane studies. No partition coefficients are available for the two other quenchers, although literature information and the structure of the molecules suggest that for bromobenzene K_p is of the same order of magnitude as for DEA, whereas for potassium iodide it should be extremely low.

An examination of Table 2 shows that the quenching efficiency by DEA in the lipid bilayer is only weakly dependent on the presence and length of the methylene chain of the pyrene derivatives. These observations lead to the conclusion that the efficiency of the diffusion-controlled quenching reaction is mainly determined by the mobility of the DEA quencher. This is also supported by the lateral diffusion coefficients of lipids and probe lipids in egg PC bilayers as measured by a variety of methods (Sackman, 1983; Jain, 1988). The reported values, in the 10^{-8}–10^{-9} $cm^2\ s^{-1}$ range, are at least one order of magnitude smaller than that derived from the present quenching experiments. The question arises as to the cause for the restricted mobility of the pyrene moiety, as compared with that of DEA. Because the behavior of Py does not differ from that of its chained derivatives (Table 3), this cannot be due to the restricted mobility imposed on the Py moiety by the chain. A feasible explanation is to attribute the relatively faster diffusion of DEA to its smaller size with respect to Py. Although the Saffman-Delbrueck theory for the diffusion of proteins in membranes (Saffman and Delbrueck, 1975) predicts only a weak dependence on size, this may be incorrect in the case of small (and noncylindrical) molecules such as Py and DEA (see Discussion by Vaz and Hallman, 1983). Alternatively, Py and DEA may exhibit a similar intramembrane lateral mobility, whereas the effective faster diffusion of DEA may be determined by a mechanism based on a fast equilibration with the water phase. This is supported by the substantial presence of DEA in the aqueous phase as indicated by the previously discussed partition coefficient.

A second conclusion, independent of any of the above

diffusion mechanisms, is that the distribution of the quencher throughout the bilayer interior is close to homogeneous. Based on the approximation (see above) that DEA is homogeneously distributed throughout the liquid-crystalline lipid phase, its effective concentration in the bilayer was calculated leading to the "effective" quenching parameters k_q (eff) given in Table 3. The value, of the order of $2 \times 10^8\ M^{-1}\ s^{-1}$, is lower by a factor of ~ 100 relative to that in acetonitrile. On the basis of an approximate value of $D \sim 10^{-5}\ cm^2\ s^{-1}$ for the diffusion coefficient in homogeneous nonviscous solutions, the corresponding parameter obtained for the diffusion of DEA in the PC bilayer is of the order of $10^{-7}\ cm^2\ s^{-1}$. The exact value of D depends on the model used for its calculation. For membranes and bilayers, two-dimensional diffusion models are most suitable (Vanderkooi and Callis, 1974; Yguerabide and Foster, 1981). We selected the Vanderkooi approach (Vanderkooi et al., 1975) as was used by Kano et al. (1981) for similar systems. Accordingly, the relative lateral diffusion coefficient D of the quenching process is given by $D = 1{,}000\,k_q$ (eff)/1.585 ZN, where k_q (eff) is the bimolecular quenching rate constant corrected for the actual concentration in the lipid bilayer, Z is the effective membrane thickness, and N is Avogadro's number. This expression leads to the data presented in Table 3 which are all in the range of 4.4×10^{-7}–$8.6 \times 10^{-7}\ cm^2\ s^{-1}$, in good agreement with the data of Kano et al. (1981) for DPPC-Dimethylaniline quenching in the fluid phase (50°C). Applying other models for two-dimensional diffusion (Yguerabide and Foster, 1981) also gives D values of the same order of magnitude (data not shown).

The results obtained with bromobenzene as quencher are consistent with the above conclusions. As shown in Table 3, the apparent quenching rate constant in the vesicle is higher than the corresponding value in a homogeneous solution by a factor of 40–160. For DEA as quencher the same parameter ratio, k_q/k_q(AC) is in the range 3–7. This discrepancy is readily accounted for by the fact that whereas with DEA the quenching process in solution is diffusion controlled, quenching by bromobenzene ($k_q \sim 10^7\ M^{-1}\ s^{-1}$) is not diffusion limited (see Tables 1–3 for the respective values of k_q in solution). For example, in the case of DEA, the increase in the effective concentration of the quencher by 100-fold under our experimental conditions is substantially compensated by the decrease in the value of k_q (eff). On the other hand, the main bilayer effect in the case of bromobenzene is due to the concentration factor. (Assuming that bromobenzene, as DEA, is quantitatively concentrated in the lipid phase.) Because k_q (eff) is not diffusion controlled, its value in the vesicle is close to that in homogeneous solutions.

The data shown in Table 1 for I^- as quencher indicate an approximately equal quenching efficiency for all derivatives. This implies substantial penetration of the iodide ion into the bilayer. The leveling off of the Stern-Volmer plots at high $[I^-]$ suggests a saturation of the lipid phase. It appears that the I^- concentration is somewhat lower in the internal regions, where the aromatic moieties of Py-dec and Py-hexdec are located, relative to, e.g., Py-val. Contrary to the cases of DEA, no estimate is available for the partition coefficient of I^- between the lipid and the aqueous phases, thus preventing calculation of an effective rate constant. It is interesting to note that the I^- quenching behavior of Py is similar to those of the long chain derivatives. Because the vertical mobility of these derivatives is assumed to be very small, this implies that no substantial vertical diffusion of $^1Py^*$ to the lipid-water interface takes place during the lifetime of the excited state. It is evident that during their excited state lifetime ($\tau = 10^{-7}$ s) Py molecules do not interact with the very high I^- concentration (1 M) in the aqueous phase. The average diffusion distance r in this time interval is of the order of $r = \sqrt{D\tau}$. An r value of <5 Å implies a limit of $D < 3 \times 10^{-8}\ M^{-1}\ s^{-1}$ for the vertical diffusion of Py in the bilayer. This value is considerably lower than that estimated above for the lateral diffusion of DEA, again demonstrating that the bilayer is an anisotropic medium and cannot be treated as a bulk.

Charge recombination process

Recombination of the radical ions, Py^- and DEA^+, generated in the present liposome systems is considerably faster than the corresponding processes in solution. For example, the diffusion-controlled recombination rate constant for Py and DEA^+ in ethanol, acetonitrile, and n-propanol is of the order of $k_r = (3 \pm 2) \times 10^{10}\ M^{-1}\ s^{-1}$. However, when treated as a second order reaction, the initial decay of Py^- and DEA^+ in the vesicle systems leads to $k_r = 10^{12}\ M^{-1}\ s^{-1}$. This value, which is unreasonably high for a pair of radical ions homogeneously distributed in the homogeneous (aqueous) solution indicates that the observed decay process takes place between radical ions confined to the bilayer region.This conclusion is in accordance with the temperature effects on the rate of the ions recombination as previously reported by us in the case of pyrene and DEA (Neumann et al., 1982). The marked increase in the decay rate around the gel to liquid-crystalline phase transition of DPPC vesicles confirms that the recombination process constitutes an intrabilayer reaction whose rate increases upon decreasing the effective internal viscosity and/or order of the membrane. A diffusion-controlled recombination of ions which escaped the membrane, reaching homogeneous distribution in the outside solu-

tion, can thus be excluded. The question arises concerning the membrane regions in which the relative diffusion of Py and DEA^+ is taking place. We have previously concluded that the quenching reaction takes place in the membrane interior. Because not only the quenching process but also the ions recombination kinetics are essentially independent of the presence (or length) of the carboxylic chain, it is evident that the recombination process is controlled by the intramembrane diffusion of the DEA^+ radical ion. The nonexponential nature of the $Py^- + DEA^+$ reaction will thus reflect the nonclassical kinetics involving a small number of reacting species caged in the vesicle bilayer. Similar problems have been treated theoretically (Darvey and Ninham, 1967; McQuarrie, 1969). In the present system a nonexponential decay is expected whenever the average number of $Py^- + DEA^+$ pairs in a single vesicle is higher than one. A detailed analysis including the effects of light intensity and liposome concentration is thus required for a quantitative description of the recombination of the ions in the vesicle. Such studies are currently in progress.

On the mechanism of exciplex, ion-pair, and triplet-state generation

Scheme II represents the main processes accounting for the charge transfer quenching of fluorescence in exciplex systems in homogeneous solutions (for a review see Mataga and Ottolenghi, 1979). $^1A^*$ denotes the excited acceptor ($^1Py^*$) and D is the donor quencher (DEA). $(^1A^*D)$ is the locally excited encounter complex and $^1(A^-D^+)^*$ represents the fluorescent exciplex. The species $[(\uparrow)A^- \ldots D^+(\downarrow)]$, in which the arrows denote the (singlet) spin configuration, represent the "solvent shared" ion pair where the ions are correlated by close range electrostatic interactions. $[A^- + D^+]$ is the "caged" ion pair in which the correlation is primarily geometrical, i.e., the geminate radical pair has not yet attained homogeneous distribution in the bulk of the solution (represented in Scheme II by $A^- + D^+$). The branching reactions at the stages of $(^1A^*D)$ and $^1(A^-D^+)^*$ are

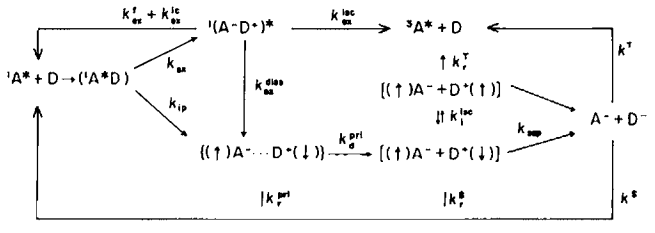

SCHEME II Major pathways in the charge transfer fluorescence quenching of typical acceptor (A)—donor (D) systems. Notations are explained in the text.

markedly affected by the solvent polarity. Thus, for pyrene-DEA in a nonpolar solvent such as hexane, the only photoproducts are the fluorescent exciplex and the pyrene triplet, implying that $k_{ex} \gg k_{ip}$ and $k_{ex}^{diss} \ll k_{ex}^f$, k_{ex}^{isc}. In a polar solvent, such as methanol, k_{ip} and k_{ex}^{diss} markedly increase, resulting in a reduced exciplex emission at the expense of ionic dissociation.

A basically different behavior is encountered in the present liposome systems. Thus, no exciplex emission is detectable in the vesicles ($\phi_{ex}^f < 0.01$) in the DEA concentration range in which the vesicles remain intact. (A fluorescence attributed to the exciplex is observed only at high [DEA] values, presumably due to a drastic change in the membrane structure.) However, in variance with homogeneous solutions, the lack of exciplex emission is not quantitatively compensated by a substantial yield of the ions. Thus, as shown previously in the case of Py/DEA (Neumann et al., 1982), and in the present work for all other Py derivatives, the relative yield of the ions in the bilayer is lower by almost a factor of 10 relative to a medium polarity solvent such as ethanol (dielectric contant: $\in = 23.9$). Because k_{ex}^{ic}, k_{ex}^f, and k_{ex}^{isc} are not markedly sensitive to the exciplex environment (Mataga and Ottolenghi, 1979), the lack of any exciplex emission in the membrane cannot be sought in a specific exciplex quenching mechanism, but rather in the prevention of its formation. Namely, by concluding that $k_{ip} \gg k_{ex}$.

A high k_{ip}/k_{ex} ratio may in principle be accounted for by a high k_{ip} value as prevailing in polar solvents such as methanol or acetonitrile ($\in > 30$). However, this possibility would be inconsistent with accumulated evidence indicating that there is a polarity gradient in the membrane interior (Thulborn, 1981) with the bilayer center having the range $\in$ = 6–10 (Vanderkooi et al., 1975; Shinitzky and Barenholz, 1978). Such values are in keeping with the relatively low polarity as indicated by the previously discussed vibronic structure of the Py fluorescence. It is in principle possible that a fast local solvation process, involving the aggregation of several water molecules around $^1(A^-D^+)^*$ and $[(\uparrow)A^- \ldots D^+(\downarrow)]$ may create an effective polar environment leading to the condition ($k_{ip} \gg k_{ex}$, $k_{ex}^{diss} \gg k_{exic} + k_{ex}^f + k_{ex}^{isc}$) as required for explaining the lack of exciplex emission. This seems highly unlikely and is not supported by studies of exciplexes in, e.g., dioxane-water mixtures which behave as homogeneous solvents of compared polarity (Orbach and Ottolenghi, unpublished data). Our present approach is to assume a "normal" dielectric constant of 5–10 for the membrane interior (Turner and Brand, 1968; Tanford, 1980) and to attribute the complete lack of exciplex emission to the inhibition of its generation by the intrinsic membrane structure. Such an effect may be due to geometrical

restrictions imposed by the anisotropic "liquid crystal" structure (Jain, 1988; Sackman, 1983) on the relative orientations of $^1Py^*$ and DEA during the quenching reaction. Thus, the exciplex yield, $\phi_{ex} = k_{ex}/(k_{ex} + k_{ip})$ due to a high effective polarity will be lowered by a low k_{ex} rather than by an increase in k_{ip}. The much higher sensitivity of k_{ex}, as compared to k_{ip}, to the relative geometrical orientation of the reacting pair is indicated by several studies of intra- and intermolecular exciplex generation (see review by Mataga and Ottolenghi, 1979; Chuang et al., 1974; Mataga et al., 1976; Okada et al., 1977; Cheung and Ware, 1983; Yorozu et al., 1981; Avnir et al. 1989). In analogy to such systems it is feasible that the lack of exciplex emission in the organized membrane medium may be attributed to restrictions imposed on the sandwich-type configurations required for excited complex formation as compared with less critical relative orientations of $^1A^*$ and D needed for the generation of the ion pair.

We should finally consider the yield of the ionic products $A^- + D^+$ in the liposome bilayer. If the lack of exciplex emission following the quenching of $^1Py^*$ by DEA is due to the effectively competing generation of the ion pair, the question arises as to why the amount of the observed ions is smaller by a factor of ~ 20 relative to that of characteristic polar solvents, such as methanol or acetonitrile. A plausible explanation is based on local order effects. As discussed above, the apparent "microviscosity" for the $^1Py^*$ + DEA recombination process as determined from the fluorescence quenching parameters is ~ 200 times larger than that of a fluid solvent such as ethanol. It has been reported that the viscosity of the medium markedly affects the yields of radical ions in exciplex systems (Orbach, 1976). For example, the relative amount of ions in the $^1Py^*$/DEA system, measured in a series of ethanol/ethylene glycol (constant $\in$) mixtures, exhibits a drop of a factor of ~ 3 over a 10-fold increase in the macroscopic viscosity of the medium. We thus suggest that the low yield of $Py^- + DEA^+$ in the liposomes is due to a "microviscosity" effect on the branching rate ratio k_r/k_d of the primarily formed ion pair $[A^- \ldots D^+]$. The effect is comparable to the medium effect on the photodissociation of molecules in viscous media (Booth and Noyes, 1960) known as the "primary" cage effect (in contrast with the "secondary" separation of the $[A^- + D^+]$ ion pair). This conclusion is in keeping with our observation (Neumann et al., 1982) that the yields of $(Py^- + DEA^+)$ following the quenching of $^1Py^*$ by DEA in DPPC liposomes increases by a factor of ~ 3, when the temperature is raised above the phase transition point of the lipid bilayer.

The results presented above (Fig. 5) indicate that the triplet amount (relative to that of the ions) generated in the quenching of pyrene and its derivatives by DEA is comparable and even higher than that observed in homogeneous polar solvents such as ethanol or acetonitrile. The mechanism of intersystem crossing (ISC) in exciplex systems have been extensively discussed by Mataga and Ottolenghi (1979). In nonpolar solvents the most general route to triplets takes place via spin-orbit interactions in the relaxed exciplex in competition with fluorescence. In polar solvents, where the exciplex yield is very small, two routes, both based on radical ion recombination, are responsible for the observed triplets (see Scheme II): a slow reaction due to the homogeneous recombination of the uncorrelated radical ions A^- and D^+ (k^T), and a fast reaction, associated with k_i^{ISC} and k_r^T (Orbach and Ottolenghi, 1975), due to triplet production in the geminate (caged) radical ion pair $[A^- + D^+]$ (undetectable under our present time resolution). The latter is induced by hyperfine interaction of the unpaired electrons (Michel-Beyerle et al., 1976; Schulten et al., 1976). It is to this geminate recombination to which we attribute the initial triplet absorption observed in the present vesicle systems earlier than ~ 50 ns after excitation. This interpretation is supported by our previous finding (Neumann et al., 1982) showing that weak magnetic field effects on the yield of $^3Py^*$, for pyrene and pyrene methanol quenched by DEA in the vesicles, are similar to those observed for Py/DEA in ethanol. Both are in keeping with the expected effect of weak magnetic fields on the rate parameter k_i^{ISC}. The essentially identical photochemical patterns observed for all molecules in Table 2 indicate that in our vesicle systems all reactions of Scheme II, including exciplex, ion-pair and triplet-state generation, take place in the interior of the lipid bilayer.

The help of Dr. Frances Stephenson (Department of Biochemistry, University of Virginia, Charlottesville, VA) with the ^{31}P NMR measurements, of Dr. E. Haas (Bar-Ilan University, Israel) with life time measurements, and of Mrs. Beryl Levene for typing the manuscript, are acknowledged with pleasure.

This work was supported in part by grant from The U.S.-Israel National Science Foundation and Public Health Service National Institutes of Health HL (17576).

Received for publication 11 June 1990 and in final form 13 December 1990.

REFERENCES

Aalbersberg, W. J., G. J. Hoijtink, E. L. Mackor, and W. P. Weijeand. 1959. The formation of hydrocarbon positive ions in strong proton donor. *J. Chem. Soc. (Lond.).* 3:3049–3054.

Anbar, M., and E. J. Hart. 1968. The Hydrated Electron. Wiley and Sons, New York.

Atik, S. S., and J. K. Thomas. 1981. Photoinduced electron transfer in organized assemblies. *J. Am. Chem. Soc.* 103:3550–3555.

Avnir, D., E. Wellner, and M. Ottolenghi. 1989. Photophysical recognition of chiral surfaces. *J. Am. Chem. Soc.* 111:2001–2003.

Bangham, A. D., J. De Gier, and G. D. Greville. 1967. Osmotic properties and water permeability of phospholipid liquid crystals. *Chem. Phys. Lipids.* 1:225–246.

Barenholz, Y., J. Suurkuusk, D. Mountcastle, T. E. Thompson, and R. L. Biltonen. 1976. A calorimetric study of the thermotropic behavior of aqueous dispersions of natural and synthetic sphingomyelins. *Biochemistry.* 15:2441–2447.

Barenholz, Y., D. Gibbs, B. J. Litman, J. Goll, T. E. Thompson, and F. D. Carlson. 1977. A simple method for the preparation of homogenous phospholipid vesicles. *Biochemistry.* 16:2806–2810.

Barenholz, Y., A. Gafni, and S. Eisenberg. 1978. Apparent microviscosity of intact and post-lipolysis ("remnant") very low density lipoprotein particles. *Chem. Phys. Lipids.* 21:179–15.

Ben Yashar, V., M. Menashe, R. L. Biltonen, M. L. Johnson, and Y. Barenholz. 1987. Interaction of trans-parinaric acid phosphatidylcholine bilayers: comparison with the effect of other fluorophores. *Biochim. Biophys. Acta.* 904:117–124.

Birks, J. R. 1970. Excimers. *In* Photophysics of Aromatic Molecules. John-Wiley and Sons Ltd., New York. 7:301–371.

Booth, D., and R. M. Noyes. 1960. The effect of viscosity on the quantum yield for iodine dissociation. *J. Am. Chem. Soc.* 82:1868–1872.

Cheung, S. T., and W. R. Ware. 1983. Exciplex photophysics. 7. Steric effects in exciplex photophysics. *J. Phys. Chem.* 87:466–473.

Chuang, T. J., R. J. Cox, and K. B. Eisenthal. 1974. Picosecond studies of the excited charge-transfer interactions in anthracene-$(CH_2)_3$-*N,N*-dimethylaniline systems. *J. Am. Chem. Soc.* 96:6828–6831.

Cullis, P. R., M. J. Hope, B. J. de Kruiff, J. Verkleij, and C. P. S. Tilcock. 1985. Structural properties and functional roles of phospholipids in biological membranes. *In* Phospholipids and Cellular Regulations J. F. Kuo, editor. CRC Press, Boca Raton, FL. 1–59.

Darvey, I. J., and B. W. Ninham. 1967. Stochastic models for second order chemical reaction kinetics. Time course of reactions. *J. Chem. Phys.* 46:(5):1626–1645.

Dong, D. C., and M. A. Winnik. 1982. The Py scale of solvent polarities solvent effects on the vibronic fine structure of pyrene fluorescence and empirical correlations E_T and *Y* values. *Photochem. Photobiol.* 35:17–21.

Galla, H. J., and W. Hartman. 1980. Excimer-forming lipids in membrane research. *Chem. Phys. Lipids.* 27:199–219.

Galla, H. J., and E. Sackmann. 1974. Lateral diffusion in the hydrophobic region of membranes: use of pyrene excimers as optical probes. *Biochim. Biophys. Acta.* 339:103–115.

Goldschmidt, C. R., M. Ottolenghi, and G. Stein. 1970. Nitrogen-laser photolysis apparatus in the nanosecond range: the excited singlet-singlet absorption spectrum of coronene. *Israel J. Chem.* 8:29–36.

Gratzel, M., K. Kalyanasundaram, and J. K. Thomas. 1974. Proton nuclear magnetic resonance and laser photolysis studies of pyrene derivatives in aqueous and micellar solutions. *J. Am. Chem. Soc.* 95:7869–7874.

Grellman, K. H., A. R. Watkins, and A. Weller. 1970. Flash photolytic investigations of electron transfer reactions in the excited state. *J. Lum.* 1–2:678–692.

Heresko, R. C., I. P. Sugar, Y. Barenholz, and T. E. Thompson. 1986. Lateral distribution of a pyrene-labeled phosphatidylcholine in phosphatidylcholine bilayers: fluorescence phase and modulation study. *Biochemistry.* 25:3813–3823.

Heresko, R. C., I. P. Sugar, Y. Barenholz, and T. E. Thompson. 1987. The lateral distribution of pyrene-labeled sphingomyelin and glucosylceramide in phosphatidylcholine bilayers. *Biophys. J.* 51:725–733.

Huang, C., J. T. Mason, F. A. Stephenson, and I. W. Levin. 1984. Raman and ^{31}P NMR spectroscopic identification of a highly ordered lamellar phase in aqueous dispersions of 1-stearoyl-2-acetyl-*Sn*-glycero-3-phosphorylcholine. *J. Phys. Chem.* 88:6454–6458.

Jain, M. S. 1988. Introduction to Biological Membranes. 2nd ed. Wiley Interscience, New York.

Kalyanasundaram, K., and J. K. Thomas. 1977. Environmental effects on vibronic band intensities in pyrene monomer fluorescence and their application in studies of micellar systems. *J. Am. Chem. Soc.* 99:2039.

Kano, K., H. Kawazumi, and T. Ogawa. 1981. Fluorescence quenching in liposomal membranes. Exciplex as a probe for investigating artificial lipid membrane properties. *J. Phys. Chem.* 85:2204–2209.

Katusim-Razem, B., M. Wong, and J. K. Thomas. 1978. The effect of micellar phase on the state and dynamics of some excited state charge transfer complexes. *J. Am. Chem. Soc.* 100:1679–1686.

Lakowicz, J. R. 1981. Fluorescence spectroscopic investigations of the dynamic properties of biological membranes. *In* Spectroscopy in Biochemistry. J. E. Bell, editor. CRC Press, Boca Raton, FL. 1:195–245.

Lichtenberg, D., and Y. Barenholz. 1988. Liposomes: preparation, characterization and preservation. *In* Methods in Biochem. Anal. D. Glick, editor. Wiley, New York. 33:337–462.

Luisetti, J., H. Mohwald, and H. J. Galla. 1979. Monitoring the location profile of fluorophores in phosphatidylcholine bilayers by the use of paramagnetic quenching. *Biochim. Biophys. Acta.* 552:519–530.

Massey, J. B., D. Hickson, H. S. She, J. T. Sparrow, D. P. Via, A. M. Gotto, and H. J. Pownall. 1984. Measurement and prediction of the rates of spontaneous transfer of phospholipids between plasma lipoproteins. *Biochim. Biophys. Acta.* 794:274–280.

Mataga, N., and M. Ottolenghi. 1979. Photophysical Aspects of Exciples in Molecular Association. R. Foster, editor. Academic Press, New York. 2:1–78.

Mataga, N., T. Okada, H. Masuhara, N. Nakashima, Y. Sakata, and S. Misumi. 1976. Electronic structure and dynamical behavior of some intramolecular exciplexes. *J. Lumin.* 12/13:159–168.

McQuarrie, D. A. 1969. Stochastic theory of chemical rate processes. *In* Advances in Chemical Physics—Stochastic Processes in Chemical Physics. K. E. Shuler, editor. Interscience Publishers. 15:149–183.

Michel-Beyerle, M. E., R. Haberkorn, W. Bube, E. Steffens, H. Schroder, H. J. Neusser, and E. W. Schlag. 1976. Magnetic field modulations of geminate recombinations of radical ions in a polar solvent. *Chem. Phys.* 17:139–145.

Nakajima, A. 1971. Solvent effect on the vibrational structures of the fluorescence and absorption spectra of pyrene. *Bull. Chem. Soc. (Jpn).* 44:3272–3276.

Neumann, S., R. Korenstein, Y. Barenholz, and M. Ottolenghi. 1982. Photo induced charge separation and recombination in exciplex systems in lipid bilayer vesicles. *Israel J. Chem.* 22:125–132.

Okada, T., T. Saito, N. Mataga, Y. Sokata, and S. Misumi. 1977. Solvent effects upon dynamic behavior of intramolecular heteroexcimers. *Bull. Chem. Soc. (Jpn).* 50:331–336.

Orbach, N. 1976. Primary processes in electronically excited states of charge-transfer systems. Ph.D. thesis. Hebrew University, Jerusalem.

Orbach, N., and M. Ottolenghi. 1975. Intersystem crossing and ionic recombination processes studied by pulsed laser excitation of charge-transfer systems. *In* The Exciplex. M. Gordon and W. R. Ware, editors. Academic Press, New York. 75–106.

Pownall, H. J., and L. C. Smith. 1989. Pyrene-labeled lipids: Versatile probes of membrane dynamics in vitro and in living cells. *Chem. Phys. Lipids.* 50:191–211.

Sackman, E. 1983. Physical foundations of molecular organization and dynamics of membranes. *In* Biophysics. W. Hoppe, W. Lokmann, H. Mark, and H. Ziegler, editors. Springer-Verlag, Berlin. 425–457.

Saffman, P. G., and M. Delbrueck. 1975. Brownian motion in biological membranes. *Proc. Natl. Acad. Sci. USA.* 72:3111–3113.

Schulten, K., H. Staerk, A. Weller, H. J. Werner, and B. Nickel. 1976. Magnetic field dependence of geminate recombination of radial ion pairs in polar solvents. *Z. Phys. Chem. (N.F.).* 101:371–390.

Shinitzky, M., and Y. Barenholz. 1978. Fluidity parameters of lipid regions determined by fluorescence polymerization. *Biochim. Biophys. Acta.* 515:367–394.

Sikaris, K. A., K. R. Thulborn, and W. H. Sawyer. 1981. Resolution of partition coefficients in the transverse plane of the lipid bilayer. *Chem. Phys. Lipids.* 29:23–36.

Stern, O., and M. Volmer. 1919. Uber die Abklingungszeit der Fluoreszenz. *Phys. Z.* 20:183–188.

Suurkuusk, J., B. R. Lentz, Y. Barenholz, R. L. Biltonen, and T. E. Thompson. 1976. A calorimetric and fluorescent probe study of the gel-liquid crystalline phase transition in small single-lamellar dipalmitoylphosphatidylcholine vesicles. *Biochemistry.* 15:1393–1401.

Tanford, C. 1980. The Hydrophobic Effect: Formation of Micelles and Biological Membranes. John Wiley and Sons, Inc., New York.

Thulborn, K. R. 1981. The use of N-(9-antroyloxy) fatty acids as fluorescent probes for biomembranes in Fluorescent Probes. Beddard, G. S., and M. A. West, editors. Academic Press, New York. 113–141.

Thomas, J. K. 1980. Radiation-induced reactions in organized assemblies. *Chem. Rev.* 80:283–299.

Tilcock, C. P. S. 1986. Lipid polymorphism. *Chem. Phys. Lipids.* 40:109–125.

Turner, D. C., and L. Brand. 1968. Quantitative estimation of protein binding site polarity. Fluorescence of *N*-arylaminonaphthalenesulfonates. *Biochemistry.* 10:3381–3390.

Vanderkooi, J. M., and J. B. Callis. 1974. Pyrene: a probe of lateral diffusion in the hydrophobic region of membranes. *Biochemistry.* 13:4000–4006.

Vanderkooi, J. M., S. Fischkoff, M. Andrich, F. Podo, and C. S. Owen. 1975. Diffusion in two dimensions: comparison between diffusional fluorescence quenching in phospholipid vesicles and in isotropic solution. *J. Chem. Phys.* 63:3661–3666.

Vaz, W., and D. Hallman. 1983. Experimental evidence against the applicability of the Saffman-Delbruc model to the translational diffusion of lipids in phosphatidylcholine bilayer membranes. *FEBS (Fed. Eur. Biochem. Soc.) Lett.* 152:287–290.

Waka, Y., K. Hamamoto, and M. Mataga. 1978. Pyrene-*N*,*N*-dimethylaniline heteroexcimer systems in aqueous micellar solutions. *Chem. Phys. Lett.* 53:242–246.

Waka, Y., N. Mataga, and F. Tanaka. 1980. Heteroexcimer systems in aqueous micellar solutions. *Photochem. Photobiol.* 32:225–340.

Weiner, J. R., R. Pal, Y. Barenholz, and R. R. Wagner. 1985. Effect of the vesicular stomatitis virus matrix protein on the lateral organization of lipid bilayers containing phosphatidylglyerol: use of fluorescence phospholipid analogues. *Biochemistry.* 24:7651–7658.

Winnik, F. M., M. A. C. Winnik, and S. Takuze. 1987. Interaction of hydroxypropylcellulose with aqueous surfactants: fluorescence probe studies and a look at pyrene-labeled polymers. *J. Phys. Chem.* 91:594–597.

Yguerabide, J., and M. C. Foster. 1981. Fluorescence spectroscopy of biological membranes. *In* Membrane Spectroscopy. E. Grell, editor. Springer Verlag, Berlin. 199–267.

Yorozu, T., K. Hayashi, and M. Irie. 1981. Chiral discrimination in fluorescence quenching. *J. Am. Chem. Soc.* 103:5480–5484.